Systematic Study of Soft X-ray Spectra of Poly(Dg)·Poly(Dc) and Poly(Da)·Poly(Dt) DNA Duplexes

Weijie Hua,[†,‡] Hiroyuki Yamane,[§] Bin Gao,[†,∥] Jun Jiang,[†] Shuhua Li,[‡] Hiroyuki S. Kato,[⊥] Maki Kawai,[⊥] Takaki Hatsui,[#] Yi Luo,[*,†] Nobuhiro Kosugi,[*,§] and Hans Ågren[*,†]

Department of Theoretical Chemistry, School of Biotechnology, Royal Institute of Technology, S-106 91 Stockholm, Sweden, School of Chemistry and Chemical Engineering, Key Laboratory of Mesoscopic Chemistry of Ministry of Education, Institute of Theoretical and Computational Chemistry, Nanjing University, Nanjing 210093, P. R. China, Institute for Molecular Science (IMS), Myodaiji, Okazaki 444-8585, Japan, Centre for Theoretical and Computational Chemistry (CTCC), Department of Chemistry, University of Tromsø, N-9037 Tromsø, Norway, The Institute of Physical and Chemical Research (RIKEN), Wako, Saitama 351-0198, Japan, and XFEL Project Head Office, RIKEN & PRESTO, JST, Hyogo 679-5148, Japan

Received: November 25, 2009; Revised Manuscript Received: March 5, 2010

In the present work, we have undertaken a combined experimental and theoretical study of X-ray spectroscopies for DNA base pairs, more precisely near-edge X-ray absorption, X-ray emission, and resonant inelastic X-ray scattering applied to poly(dG)·poly(dC) and poly(dA)·poly(dT) DNA duplexes. We have derived several conclusions on the nature of these X-ray spectra: the stacking of pairs has very little influence on the spectra; the spectra of a DNA composed of mixed Watson−Crick base pairs are well reproduced by linear combinations of GC and AT base pairs involved; the amine and imine nitrogens show noticeable differences as building blocks in the absorption, emission, and resonant emission spectra. The calculated spectra are in good agreement with experimental results. The ramifications of these conclusions for the use of X-ray spectroscopy for DNA are discussed.

Introduction

The application of X-ray spectroscopy in materials research is often motivated by its potential to specify the constituting atomic elements and the chemical and electronic structure of the sample under study. Radiative transitions in the soft X-ray range connect well localized core orbitals with delocalized molecular orbitals or bands, and have therefore the inherent capability to map out the local electronic structure of the orbitals or bands around the core hole in question. Multiple core spectra of the same compound, either by different elements or by the same element in different chemical positions, can in favorable cases provide a full mapping of the electronic structure, and can also give evidence of the chemical positions of the various elements. This has led to many applications of X-ray spectroscopy including the determination of the electronic structure and orientation of molecules in the solid state and absorbed on surfaces. Qualitatively, it is possible to correlate specific spectral features with functional groups and, in some cases, individual bonds, such that the total spectrum can be considered as a linear combination of elementary spectra. This conceptual approach, named the "building block principle",[1−5] provides a useful starting point for the interpretation of spectra of very complicated molecules. However, there are certainly limits to the building block approach. Delocalization of electronic charge across multiple functional groups leads to new molecular orbitals (MO) combining the properties of the conjugated groups. In such cases, the spectral features of the individual groups can be changed and new features may appear.

One theme of this work is to explore the limits of the conceptual picture briefly reviewed above in the case of DNA and to find out if "building blocks" are suitable for the description of DNA X-ray spectra. Our work is in a general sense motivated by the importance of DNA and of the search for new technology for sequences of its genetic code. It also extends earlier experimental and computational studies of the near-edge X-ray absorption fine structure (NEXAFS) spectra of amino acids and small polypeptides.[6−9] These previous measurements demonstrated the ability of NEXAFS spectroscopy to identify particular amino acids and to use their characteristic features for chemical mapping in soft X-ray spectro-microscopy. It was found that amino acids with aromatic side chains have distinct spectra with signatures that do not change much during the peptide bond formation. Subsequent computational analysis helped to identify the origin of individual peaks and motivated a more extended analysis of the experimental data and their spectroscopic assignments. The present work is further motivated by the earlier series of X-ray measurements of polynucleotides.[10−15]

We present a comprehensive spectral interpretation of guanine(G)·cytosine(C) pair and adenine(A)·thymine(T) pair DNA duplexes, by both experiment and theoretical calculations. We also extend from pure X-ray absorption to two other types of X-ray spectroscopy: X-ray emission spectroscopy (XES) and resonant inelastic X-ray scattering (RIXS) spectroscopy. We will focus on spectra of the nitrogen element, which is involved only in the nucleobases, and therefore give the clearest fingerprint of the DNA. Our work should be qualified in view of earlier efforts in the area, with the first NEXAFS work on DNA being

* To whom correspondence should be addressed. E-mail: luo@theochem.kth.se (Y.L.); kosugi@ims.ac.jp (N.K.); agren@theochem.kth.se (H.Å.).
[†] Royal Institute of Technology.
[‡] Nanjing University.
[§] Institute for Molecular Science.
[∥] University of Tromsø.
[⊥] The Institute of Physical and Chemical Research.
[#] XFEL Project Head Office.

10.1021/jp911199e
Published on Web 05/03/2010

the one by Kirtley[10] who compared experimentally the N 1s spectra of DNA, bases, nucleotides, polynucleotides, and other related samples, and analyzed the influence of different groups to the spectra. MacNaughton et al. analyzed the influence of the environment in different DNA samples by X-ray absorption spectroscopy (XAS) and XES,[11] and gave the XAS and RIXS spectra of DNA with and without metal ions.[12] Kato and co-workers[13,15] studied NEXAFS of DNA duplexes with and without the presence of iodine.

We note that most of the related theoretical X-ray investigations have addressed small molecules: bases,[14,16] base pairs,[17,18] metal combined base pairs,[12] or dinucleotides.[14] To the best of our knowledge, there is so far a lack of computational studies on X-ray spectra for larger molecules than those cited with reference to real DNA. This state of affairs give impetus for the present contribution where we carry out a combined experimental and theoretical study of the DNA duplexes. First, we tune different incident photon energies to resonate with specific transitions and measure the RIXS spectra. Second, with the help of the equivalent core hole (ECH) approximation,[19,20] we study a series of stacked base pairs with increasing number of units in order to explore the convergence of NEXAFS, XES, and RIXS spectra with respect to the number of base pairs. Moreover, our theoretical calculations provide detailed interpretation of the experimental spectra of DNA.

Experimental Section

Sample Preparation. For the soft X-ray experiments, we prepared thick DNA duplex films of poly(dG)·poly(dC) and poly(dA)·poly(dT) DNA (Amersham Biosciences Ltd., length = 0.5−2.9 μm). The DNA duplexes were diluted with deionized water (17.8 MΩ·cm) to a concentration of 1.25 mg/mL. The solutions were casted onto the SiO_2/*p*-Si(111) substrates. The film thickness is about 100−200 nm. These samples are almost the same as those measured at the previous resonant photoemission experiments.[13] Note that we confirmed in our prior experiment that there was no difference in the XAS spectra between the DNA sample and a water-contained DNA sample upon cooling. Therefore, the effect of the water inclusion is negligible, although few water molecules may exist even in the ultrahigh vacuum (UHV) condition.

NEXAFS and XES/RIXS. The soft X-ray experiments (NEXAFS and XES/RIXS) were performed at an in-vacuum soft X-ray undulator beamline BL3U[21] at the storage ring UVSOR-II (IMS, Okazaki). The NEXAFS spectra were measured by the highly efficient fluorescence-yield method using an MCP assembly with the center hole (F2223-21SH, Hamamatsu Photonics K.K.). The XES/RIXS spectra were measured using a newly developed XES/RIXS apparatus based on a highly efficient transmission-grating spectrometer.[22] All measurements were performed at room temperature (300 K). In the present experiments, we set the incident energy resolution for NEXAFS and XES/RIXS to 0.1 eV and 0.4−0.5 eV at $h\nu$ = 400 eV, respectively.

For the XES/RIXS spectra, we need a small photon spot size [40 μm (horiz.) × 20 μm (vert.)] and long accumulation times (60−90 min per 1 spectrum). Even in the photon flux of 10^{11} ph/s range, the XES/RIXS spectra show evidence for radiation damage within 30−60 min of X-ray irradiation. In order to avoid radiation damage, the X-ray irradiated spot was continuously changed by scanning the sample at the rate of 20 μm/min during the measurements.

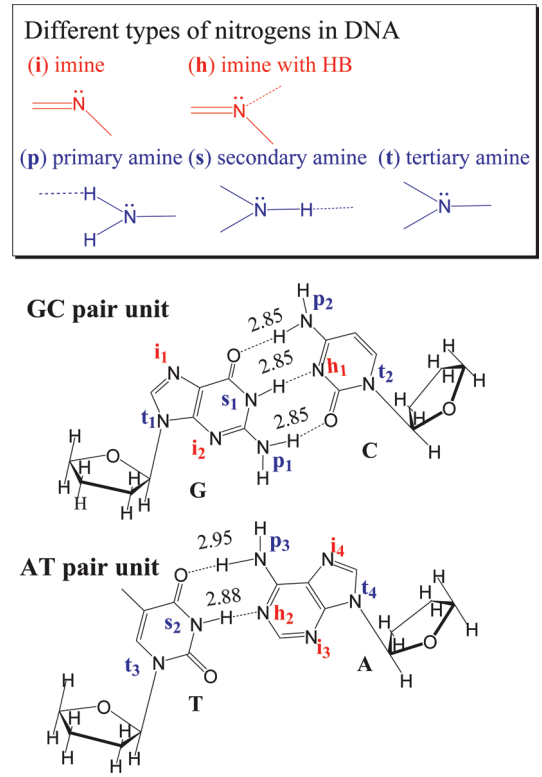

Figure 1. Calculation models with one base pair unit. Different types of nitrogens and HB lengths (in Å) are labeled.

Computational Methods

Models. We first choose the GC and AT base pair structures from the SPARTAN library.[23] As shown in Figure 1, we further neglect the methylene connected phosphate group as well as the hydroxyl group in the ribose ring and replace them with hydrogens. Such a modification is called for because of the complexity of the calculations and is based on the localized property of X-ray spectroscopies, and is a posteriori motivated by the computational results (see below). Furthermore, point tests have shown that such a modification does not significantly influence the NEXAFS spectra. Next, type B DNA duplexes of $(gc)_n$ and $(at)_n$ (n = 1, 2, 4, 6) are constructed by rotation (by twist angle of 36°) and translation (by pitch distance of 3.375 Å) of the base pair coordinates. Here, we have used the notation, for example, $(gc)_2$ for the d(GCGC)·d(CGCG) [i.e., (dG-dC)$_2$·(dC-dG)$_2$)] duplex which contains four GC pairs. NEXAFS, XES, and RIXS spectra were calculated for these series of models with increasing sizes without geometry relaxation. The different types of nitrogen atoms, illustrated in the figures, were addressed. Usually, the nitrogens in DNA are classified as two types: imine and amine nitrogens. According to their local bonding, we further divide the former into normal imine nitrogens (denoted by *i*) and imine nitrogens with hydrogen bond (HB) (*h*) subtypes; the latter is divided into primary (*p*), secondary (*s*), and tertiary (*t*) amine nitrogens subtypes. We will analyze the contribution from each nitrogen to explore the dependence of the spectra on structure. Such a classification aims to pay special attention to the influence of the hydrogen bonds between the paired bases.

NEXAFS. We calculated the N 1s NEXAFS spectra for both base pairs and the $(gc)_n$, $(at)_n$ duplexes at the B3LYP[24] level with the ECH approximation using the GAUSSIAN 03[25] package. The IGLO-III basis set[26] is chosen for the excited atom, and the 6-31G basis set for the remaining atoms. With the MO

coefficients and multipole moments provided, the spectra are then calculated by using the BIONANO-LEGO[27] code. We applied the ECH approximation, also referred as the Z+1 approximation, meaning that an atomic nucleus is replaced by the next element in the periodic table while the number of electrons remains unchanged. It can well reproduce the core hole state and is widely used for the calculation of NEXAFS spectra for various types of systems such as nanoscale molecules, like phthalocyanine[28] and fullerene,[29] and nanomaterials, like single-walled carbon nanotubes.[30]

Each obtained core hole spectrum has been calibrated and labeled by the relative position of the ionization potential (IP). Using the Δ Kohn−Sham (ΔKS) approach,[31,32] we calculate an accurate value of the first excitation energy, corresponding to the 1s→LUMO (lowest unoccupied molecular orbital) transition, and the IP. In this approach, the first excitation energy is calculated as the energy difference of the core excited state (i.e., 1s→LUMO) and the ground state (GS), as in the following equation:

$$\varepsilon_{1s\rightarrow LUMO} = {}^{N}E_{1s\rightarrow LUMO} - {}^{N}E_{GS}$$

Similarly, the IP is calculated as the energy difference of the core ionized state [i.e., full core hole (FCH)] and the GS:

$$IP = {}^{N-1}E_{FCH} - {}^{N}E_{GS}$$

This approach considers relaxation of the core hole state and thus gives ionization energies with high precision. In practice, we do this directly only for the two base pairs, while for the duplex sequences the same shift value is assumed. Additionally, for these two base pairs, we also calculate the NEXAFS spectra with the FCH approach in order to validate our ECH results. These FCH calculations are all carried out at the density functional theory (DFT) level with the StoBe package.[33] The gradient corrected Becke[34] (BE88) and Perdew[35] (PD86) functionals are chosen for the exchange and correlation parts, respectively. Concerning orbital basis sets, we use the IGLO-III basis set[26] for the excited atom and triple-ζ plus valence polarization (TZVP) basis set for the rest; miscellaneous auxiliary basis sets are also set for all atoms; an optional model core potential is also added for the non-excited nitrogens to facilitate the self-consistent field (SCF) convergence.[36] Finally, a correction term of +0.3 eV for differential relativistic effects associated with the removal of one electron from the N 1s orbital is applied, and the stick spectra are Lorentzian convoluted with full-width-at-half-maximum (FWHM) set at 0.2 eV.

XES and RIXS. XES and RIXS calculations are performed with the ground state wave functions referring to the final state rule. For XES, we consider transitions to the 1s orbitals of all nitrogens. The RIXS spectra are obtained for the two types of nitrogens when decomposing all the contributions from the amine and imine nitrogens. Stick spectra are convoluted with a FWHM of 0.5 eV. Such a prediction cannot give an accurate absolute value for the energies due to the neglect of the core hole relaxation effects, and the calculated spectra are therefore uniformly shifted about 10 eV to accord with experiment. The calculations are performed at the B3LYP/6-31G level using the GAUSSIAN 03 program. The spectra are also calculated by using the BIONANO-LEGO program.[27]

Results and Discussion

NEXAFS. The total NEXAFS spectra at the nitrogen 1s edges for the GC-based and AT-based models are plotted in Figure 2, while the detailed contributions from different nitrogens are shown in Figure 3, using $(gc)_6$ and $(at)_6$ as examples. Figure 2 can be divided into three regions. Regions I (less than 400.2 eV) and II (between 400.2 and 402.4 eV) correspond to 1s→π^* transitions from the imine and amine nitrogens, respectively. Region III (beyond 402.4 eV) is due to 1s→σ^* transitions. In both panels, the calculated spectra match quite well with the experimental ones. By comparing the series of models, one can recognize a quick convergence with the system size. Region I remains almost unchanged with respect to the increase of the base pairs, while region II shows a slight length dependence. This demonstrates that the stacking effect among the constituting base pairs does not have an effective influence on the NEXAFS spectra, something that has important consequences for using NEXAFS in DNA analysis. Furthermore, the FCH spectrum of either base pair matches quite well with the ECH one which supports the reliability of the ECH results.

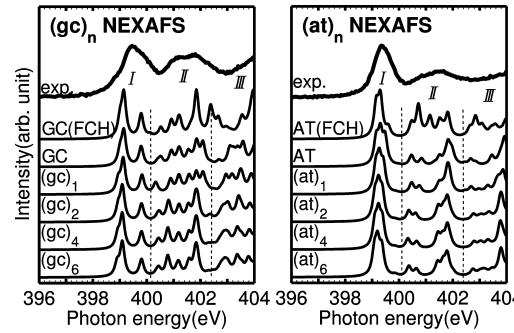

Figure 2. N 1s NEXAFS spectra calculated from different sizes of models. They are all shifted by +0.2 eV for better comparison with experiment.[13]

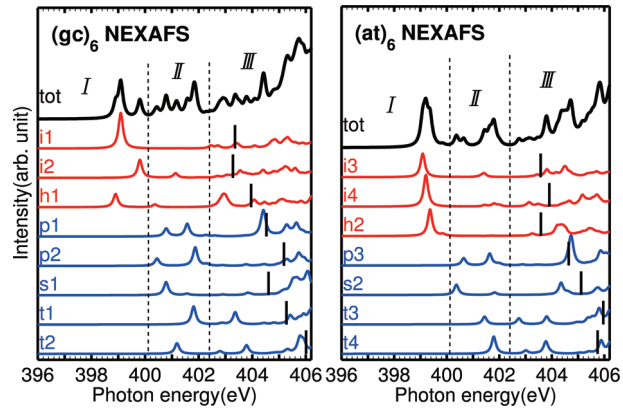

Figure 3. Atom-specific N 1s NEXAFS theoretical spectra of $(gc)_6$ and $(at)_6$. Bars denote IPs which are "borrowed" from corresponding nitrogen from GC and AT base pairs. The spectra and IPs are shifted by +0.2 eV for better comparison with experiment.[13]

Now we are at the stage to analyze the contribution from each individual nitrogen. We also consider the three regions one by one. Region I origins in transitions to LUMOs. In the left panel of Figure 3, i_1 and h_1 have close first absorption energies which both contribute to the peak around 399.1 eV (399.1 and 398.9 eV). i_2 contributes at around 399.8 eV, while in the right panel the three imine nitrogens all have the first absorption energies at 399.2 eV (399.1, 399.2, and 399.4 eV) which creates a strong sharp peak in this position. The hydrogen bonded nitrogen (*h*) does not show any significant difference with those without HB (*i*). For region II, the low-lying

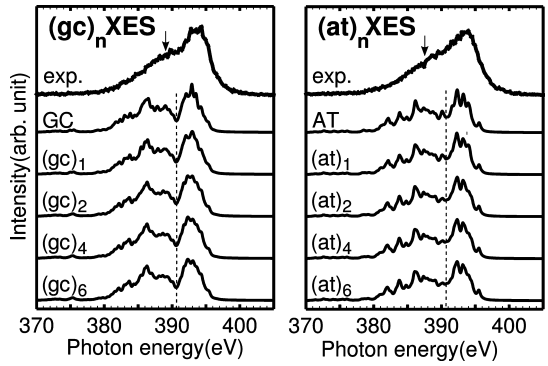

Figure 4. Normal N 1s XES of DNA duplexes by experiment (incident photon energy $h\nu_i$ =410 eV) and by calculations with different sizes of models. The calculated spectra are shifted by +10 eV to match with experiment.

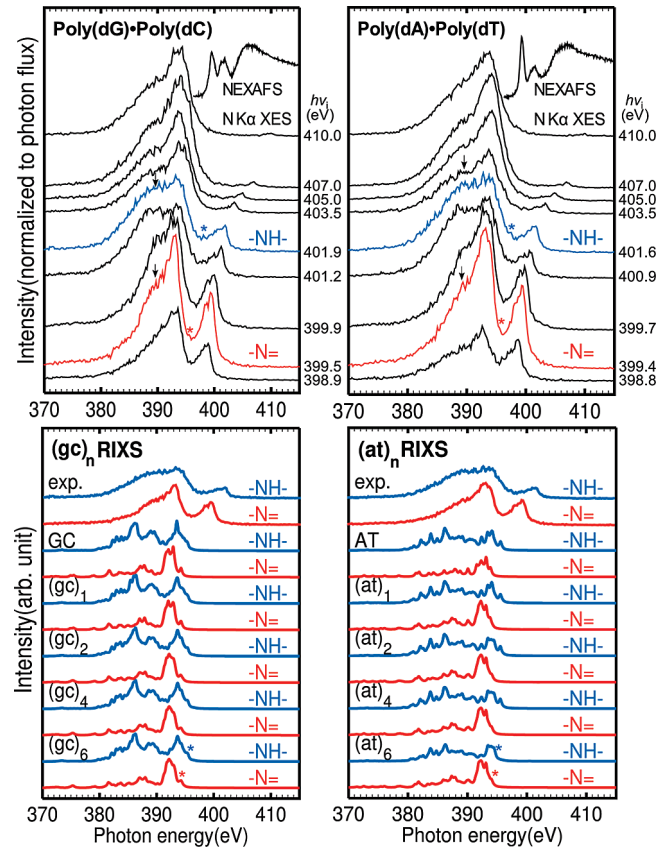

Figure 5. Top: Experimental XES spectra of GC- and AT-DNA films. Bottom: N 1s RIXS spectra of DNA duplexes by experiments and by calculations with different sizes of models. The calculated spectra are shifted by +10 eV to match with experiment. Stars denote the highest occupied molecular orbitals.

absorption transitions (to LUMOs and LUMO+1's) of amine make up for the major contribution, but the imine nitrogens also have weak absorption in this region. Similar to the imine case, the spectra do not show significant type dependence among the primary, secondary, or tertiary amine nitrogens. In region III, the IP of each nitrogen is also shown covering the energy interval between 403.3 and 406.0 eV. For both the $(gc)_6$ and $(at)_6$ cases, all amine nitrogens show higher IPs than the imine nitrogens. Energies near and beyond the IPs are continuum regions which cannot be analyzed directly through our calculations, as our line spectra do not possess proper normalization in the continuum region.

XES. In Figure 4, we display the experimental and calculated normal X-ray emission spectra. Both experimental curves exhibit a peak at 394 eV and a preshoulder at around 389 eV (or 388 eV) (denoted by arrows), and they do not show evident visible difference. The theoretical spectra also cover almost the same range. Generally, one can see that the spectra quickly converge for either series. In either panel, a clear distinction of the two regions divided by 391 eV can be seen. These two regions can approximately be assigned to the two experimental peaks, respectively. In addition, they also show more detailed properties: in $(gc)_n$ series, the spectra are characterized by a broad peak around 386 eV and a sharp peak around 393 eV; the $(at)_n$ sequences have more disperse features and exhibit multiple peaks, which can be also seen in the line shapes of the experimental XES spectra. It is not easy to further disentangle the two regions, as too many transitions appear in either region. One can, however, distinguish the contributions from the imine and amine nitrogens by studying the RIXS spectra, as shown below.

RIXS. The experimental and theoretical RIXS spectra are shown in Figure 5. In the experimental panel, one finds that the imine and amine groups can be distinguished as labeled by −N═ and −NH−, respectively. The imine nitrogens resonate with an incident photon energy $h\nu_i$ at 399.5 eV (399.4 eV) for GC-DNA (AT-DNA). Either DNA sample exhibits two inelastic features: one shoulder (denoted by arrow for visualization) at 390 eV and one peak at 393 eV. On the other hand, the amine nitrogens resonate with a higher $h\nu_i$ at 401.9 eV (401.6 eV) for GC-DNA (AT-DNA). At this amine site, for both GC and AT pairs, the peak structure appears at different photon energy (394 eV) with weak intensity as compared to that appearing at the imine site.

Quick convergence is observed in the theoretical spectra for each series. They match well with the experiment, and the difference between the imine and amine nitrogens becomes distinguishable. In the $(gc)_n$ sequences, the imine nitrogen spectra are characterized by a weak double peak at 387−388 eV and a sharp peak at 392.2 eV, while the amine nitrogen spectra clearly show three peaks at 386.1, 388.9, and 393.6 eV. In the $(at)_n$ sequences, the spectra are more disperse than in $(gc)_n$, as in the XES case. The imine nitrogen spectra are characterized also by a weak double peak feature at 387−388 eV and a sharp double peak around 392.2−393.2 eV, while the amine nitrogen spectra show a sharp peak at 393−395 and many small peaks in the region below. To conclude, through RIXS we get clear signatures of the imine and amine nitrogens of DNA.

Theoretical calculations can provide more detailed information about molecular orbitals. For instance, Figure 6 shows calculated highest occupied molecular orbitals (HOMOs) of ground state $(gc)_6$ and $(at)_6$ molecules. It is interesting to see that both HOMOs are delocalized over 6 and 4 base pairs, respectively, in $(gc)_6$ and $(at)_6$ but only restricted on the purine nucleobases, showing roughly a single helix shape. It explains why the HOMO only presents in the RIXS spectrum from the imine nitrogens. This finding could also be helpful for understanding electron/charge transport processes in DNA.[37,38] Moreover, the HOMO of the $(gc)_6$ has slightly higher energy (around 0.9 eV) than that of the $(at)_6$, which supports the early observation that the guanine often contributes to the HOMO of a mixed DNA.[14]

Finally, we briefly discuss the line shape of the elastic band in the experimental RIXS spectra. As seen in Figure 5, this band

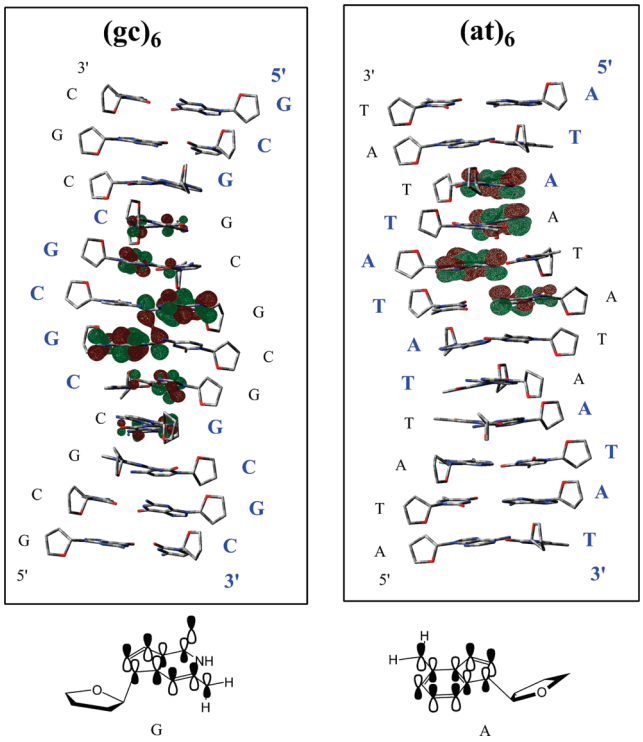

Figure 6. Isosurface of HOMO for both $(gc)_6$ and $(at)_6$ (hydrogen atoms not shown) with contour = 0.02.

shows an asymmetric line shape with a low-energy tail structure, in particular at the imine site. This tail structure may originate from the recombination emission due to the fast motion of hydrogen bonded protons between the pairs, which depends on the degree of localization of the excited state. The observation of the low-energy tail structure indicates that the excited π^* state at the imine site is strongly localized, which agrees well with the scenario of a charge hopping transport mechanism in the GC and AT pairs proposed by the previous resonant photoemission work of Kato et al.[13]

Conclusion

We have studied the application of three X-ray spectroscopies, near-edge X-ray absorption fine structure (NEXAFS), X-ray emission (XES), and resonant inelastic X-ray scattering (RIXS) spectroscopies, on poly(dG)·poly(dC) and poly(dA)·poly(dT) DNA duplexes using experimental and computational techniques. We have found that the effect of stacking between pairs in either of the systems is of little consequence for the spectra and that these with a good approximation can be represented just by one of its constituting base pairs. We can furthermore conclude that, for DNA composed by mixed Watson−Crick base pairs, the X-ray spectra are well reproduced by linear combinations of those of GC and AT base pairs according to their relative proportions. The theoretical total spectra calculated from summation of individual contributions are in good agreement with experimental measurements, indicating that the "building block principle" works well for DNA systems. Furthermore, the individual NEXAFS contributions from different types and subtypes of nitrogens are analyzed. The amine and imine nitrogens show noticeable differences from each other in the NEXAFS and RIXS spectra and in the chemical shifts of their ionization potentials, while in either type there is no clue to show subtype dependence. These conclusions will have wide ramification for the use of X-ray spectroscopy in further studies of electronic and conformational structures and properties of DNA systems.

Acknowledgment. This work was supported by the Swedish Foundation for International Cooperation in Research and Higher Education, through the contract Dnr IG2008-2026 for collaboration between the Royal Institute of Technology, Stockholm, and the Institute of Molecular Science, Okazaki. Y.L. and H.Å. acknowledge the support of Swedish Research Council (VR) and the Swedish National Infrastructure for Computing (SNIC). S.L. acknowledges the support of the National Basic Research Program (Grant No. 2004CB719901) and the National Natural Science Foundation of China (Grant Nos. 20625309 and 20833003). W.H. acknowledges the support of the China Scholarship Council (CSC).

References and Notes

(1) Stöhr, J. *NEXAFS spectroscopy*; Springer-Verlag: Berlin, Heidelberg, New York, 1992.
(2) Hitchcock, A.; Tronc, M.; Modelli, A. *J. Phys. Chem.* **1989**, *93*, 3068.
(3) Jordan-Sweet, J.; Kovac, C.; Goldberg, M.; Morar, J. *J. Chem. Phys.* **1988**, *89*, 2482.
(4) Pettersson, L.; Ågren, H.; Schürmann, B.; Lippitz, A.; Unger, W. *Int. J. Quantum Chem.* **1977**, *63*, 749–765.
(5) Plashkevych, O.; Yang, L.; Vahtras, O.; Ågren, H.; Petterson, L. G. M. *Chem. Phys.* **1997**, *222*, 125–137.
(6) Carravetta, V.; Plashkevych, O.; Ågren, H. *J. Chem. Phys.* **1998**, *109*, 1456.
(7) Plashkevych, O.; Carravetta, V.; Vahtras, O.; Ågren, H. *Chem. Phys.* **1998**, *232*, 49.
(8) Yang, L.; Plashkevytch, O.; Vahtras, O.; Carravetta, V.; Ågren, H. *J. Synchrotron Radiat.* **1999**, *6*, 708.
(9) Kaznacheyev, K.; Osanna, A.; Jacobsen, C.; Plashkevych, O.; Vahtras, O.; Agren, H.; Carravetta, V.; Hitchcock, A. P. *J. Phys. Chem. A* **2002**, *106*, 3153.
(10) Kirtley, S. M.; Mullins, O. C.; Chen, J.; van Elp, J.; George, S. J.; Chen, C.; O'Halloran, T.; Cramer, S. P. *Biochim. Biophys. Acta* **1992**, *1132*, 249.
(11) MacNaughton, J. B.; Moewes, A.; Lee, J. S.; Wettig, S. D.; Kraatz, H.; Ouyang, L. Z.; Ching, W. Y.; Kurmaev, E. Z. *J. Phys. Chem. B* **2006**, *110*, 15742.
(12) MacNaughton, J. B.; Kurmaev, E. Z.; Finkelstein, L. D.; Lee, J. S.; Wettig, S. D.; Moewes, A. *Phys. Rev. B* **2006**, *73*, 205114.
(13) Kato, H. S.; Furukawa, M.; Kawai, M.; Taniguchi, M.; Kawai, T.; Hatsui, T.; Kosugi, N. *Phys. Rev. Lett.* **2004**, *93*, 086403.
(14) Harada, Y.; Takeuchi, T.; Kino, H.; Fukushima, A.; Takakura, K.; Hieda, K.; Nakao, A.; Shin, S.; Fukuyama, H. *J. Phys. Chem. A* **2006**, *110*, 13227.
(15) Furukawa, M.; Kato, H. S.; Taniguchi, M.; Kawai, T.; Hatsui, T.; Kosugi, N.; Yoshida, T.; Aida, M.; Kawai, M. *Phys. Rev. B* **2007**, *75*, 045119.
(16) MacNaughton, J.; Moewes, A.; Kurmaev, E. Z. *J. Phys. Chem. B* **2005**, *109*, 7749.
(17) Ekström, U.; Norman, P.; Carravetta, V.; Ågren, H. *Phys. Rev. Lett.* **2006**, *97*, 143001.
(18) Healion, D. M.; Schweigert, I. V.; Mukamel, S. *J. Phys. Chem. A* **2008**, *112*, 11449.
(19) Davis, D. W.; Shirley, D. A. *Chem. Phys. Lett.* **1972**, *15*, 185.
(20) Plashkevych, O.; Privalov, T.; Ågren, H.; Carravetta, V.; Ruud, K. *Chem. Phys.* **2000**, *260*, 11.
(21) Hatsui, T.; Shigemasa, E.; Kosugi, N. *AIP Conf. Proc.* **2004**, *705*, 921.
(22) Hatsui, T.; Setoyama, H.; Shigemasa, E.; Kosugi, N. *J. Electron Spectrosc. Relat. Phenom.* **2005**, *144−147*, 1059.
(23) *SPARTAN'02*; Wavefunction Inc.: Irvine, CA, 2002.
(24) Lee, C.; Yang, W.; Parr, R. G. *Phys. Rev. B* **1988**, *37*, 785.
(25) Frisch, M. J. et al. *GAUSSIAN 03*, revision D.01; Gaussian, Inc.: Wallingford, CT, 2004.
(26) Kutzelnigg, W.; Fleischer, U.; Schindler, M. *NMR Basic Principles and Progress*; Springer Verlag: Heidelberg, 1990; Vol. 23, p 165.
(27) Gao, B.; Jiang, J.; Liu, K.; Luo, Y. *BIONANO-LEGO*, version 2.0; Royal Institute of Technology: Sweden, 2008.
(28) Brena, B.; Luo, Y.; Nyberg, M.; Carniato, S.; Nilson, K.; Alfredsson, Y.; Åhlund, J.; Mårtensson, N.; Siegbahn, H.; Puglia, C. *Phys. Rev. B* **2004**, *70*, 195214.

(29) Nyberg, M.; Luo, Y.; Triguero, L.; Pettersson, L. G. M.; Ågren, H. *Phys. Rev. B* **1999**, *60*, 7956.
(30) Gao, B.; Wu, Z. Y.; Ågren, H.; Luo, Y. *J. Chem. Phys.* **2009**, *131*, 034704.
(31) Triguero, L.; Plashkevych, O.; Pettersson, L. G. M.; Ågren, H. *J. Electron Spectrosc. Relat. Phenom.* **1999**, *104*, 195.
(32) Bagus, P. *Phys. Rev.* **1965**, *139*, A619.
(33) Hermann, K. et al. *StoBe-deMon*, version 3.0; 2007.
(34) Becke, A. D. *Phys. Rev. A* **1988**, *38*, 3098.
(35) Perdew, J. P. *Phys. Rev. B* **1986**, *33*, 8822.
(36) Hermann, K.; Pettersson, L. G. M. *Documentation for STOBE2007*; Berlin, Stockholm, 2007.
(37) Sakamoto, S.; Ohmachi, Y.; Tomiya, M. *J. Phys.: Conf. Ser.* **2007**, *61*, 1012.
(38) Wagenknecht, H.-A. Photoinduced Electron Transport in DNA: Toward Electronic Devices Based on DNA Architecture. In *NanoBioTechnology: BioInspired Devices and Materials of the Future*; Shoseyov, O., Levy, I., Eds.; Humana Press Inc.: Totowa, NJ, 2008; Chapter 5, pp 89−106.

JP911199E